Polymer Testing 128 (2023) 108205

Contents lists available at ScienceDirect

Polymer Testing

journal homepage: www.elsevier.com/locate/polytest

Structural reversible adhesives based on thiol-epoxy vitrimers

Adrià Roig [a], Laura Molina [b], Àngels Serra [a], David Santiago [b,c,**], Silvia De la Flor [b,*]

[a] Universitat Rovira i Virgili, Department of Analytical and Organic Chemistry, C/ Marcel·lí Domingo 1, 43007, Tarragona, Spain
[b] Universitat Rovira i Virgili, Department of Mechanical Engineering, Av. Països Catalans 26, 43007, Tarragona, Spain
[c] Eurecat – Chemical Technology Unit, C/ Marcel·lí Domingo 2, 43007, Tarragona, Spain

ARTICLE INFO

Keywords:
Thiol-epoxy
Covalent adaptable networks
Vitrimers
Functional adhesives
Reversible adhesives

ABSTRACT

This work presents a family of functional adhesives based on covalent adaptable networks (CANs). Low-cost and commercially available monomers, including diglycidyl ether of bisphenol A, pentaerythritol tetrakis (3-mercapto propionate) and dipentaerythritol hexakis (3-mercapto propionate), were cured using a base catalyst to produce highly cross-linked materials. The catalyst selection and the study of the curing reaction were performed using differential scanning calorimetry (DSC) and Fourier-transform infrared spectroscopy (FTIR). The catalyst was chosen for better feasibility of industrial production, characterized by short curing times and relatively low temperatures. Thermal stability and thermomechanical properties of the final materials were evaluated through thermogravimetry (TGA) and dynamic mechanical thermal analysis (DMTA), respectively, revealing glass transition temperatures (T_g) higher than 50 °C. Stress relaxation tests were conducted to investigate the vitrimeric behaviour of the polymers, which exhibited an Arrhenius-type dependence of relaxation times on temperature. Importantly, both materials demonstrated impressive creep resistance up to 70 °C, indicating their suitability for use at elevated service temperatures. Tensile and lap-shear tests were also performed, revealing high lap-shear strength values (up to 16 MPa) comparable to those of commercial adhesives. Furthermore, these vitrimers displayed remarkable properties such as shape memory, shape reconfiguration, and self-welding capabilities, underscoring their excellent potential for a wide range of highly demanding applications in industrial production.

1. Introduction

Thermosets are widely recognized for their diverse range of applications in various sectors, including coatings [1], automobile manufacturing [2], and the optoelectronic industry [3]. However, their relevance in the field of adhesion stands out as one of their most significant contributions [4,5]. With the growing demand for adhesive bonding in industrial settings, there is a pressing need for novel adhesive materials to serve as viable alternatives to mechanical joints. Extensive research has been conducted in recent years to explore different types of adhesive materials [6–9]. Typically, these adhesives are based on thermosetting polymers known for their excellent mechanical performance. However, their crosslinked structure renders them non-recyclable and non-reprocessable, leading to significant environmental concerns. To address this limitation, the academic and industrial communities have directed their attention towards developing covalent adaptable networks (CANs). These materials combine the desirable mechanical properties of thermosets with the reprocessability and recyclability of thermoplastics [10]. CANs incorporate dynamic covalent bonds that impart mobility to the network, enabling a transition from a viscoelastic solid to a fluid-like plastic flow in response to external stimuli, often temperature [11]. Several types of CANs are described in the literature, with the nature of their dynamic chemistry influencing the final molecular architecture. Among CANs, vitrimers hold particular significance [12–18]. These materials exhibit a unique exchange mechanism between dynamic bonds that occurs in a concerted manner, meaning that the breakage and the formation of bonds occur simultaneously without any intermediate state. This mechanism maintains a constant crosslinking density, resulting in a gradual decrease in viscosity with temperature, following an Arrhenius law akin to vitreous silica [19,20]. Extensive efforts have been dedicated to the development of vitrimers, particularly those based on transesterifications, which were first described by Prof. Leibler in 2011 [20–24]. Owing to their exceptional properties, vitrimeric materials find applications across various

* Corresponding author.
** Corresponding author. Universitat Rovira i Virgili, Department of Mechanical Engineering, Av. Països Catalans 26, 43007 Tarragona, Spain.
E-mail addresses: david.santiago@eurecat.org (D. Santiago), silvia.delaflor@urv.cat (S. De la Flor).

https://doi.org/10.1016/j.polymertesting.2023.108205
Received 2 July 2023; Received in revised form 23 August 2023; Accepted 10 September 2023
Available online 12 September 2023

industrial domains. The temperature-dependent viscosity of vitrimers, following an Arrhenius-type relationship and the presence of exchangeable bonds near the surfaces, enables their welding by forming of interfacial crosslinks between polymer interfaces at high temperatures. This characteristic makes vitrimers highly promising for future adhesive applications in the industrial sector. As the exchangeable links are not consumed but rather exchanged during the welding process, a joint can be reformed without modifying the surface of vitrimers, simply by applying the appropriate stimulus while the two surfaces are in contact [25]. Moreover, a joint can be disassembled by raising the temperature above the topology freezing temperature (or in some cases above T_v and T_g) and pulling the adherents apart without incurring any damage or loss of integrity. Although the industrial utilization of vitrimers is still in its early stages, several examples of adhesive polymers are described in the existing literature. Verge et al. prepared a cardanol-based polybenzoxazine vitrimer containing disulfide bonds [26]. This vitrimer exhibited adhesive properties with short curing times, even at low temperatures, and demonstrated the ability to be recycled and reconfigured due to its short relaxation times and low activation energy. However, despite its reversibility and reprocessability, the adhesive properties of the obtained material were weaker compared to commercially available options. Sridhar and co-workers reported on thermally reversible crosslinked adhesives based on dissociative Diels-Alder networks [27]. These adhesives could be repeatedly re-used through heating/cooling cycles without using solvents during preparation or reutilization. Furthermore, they exhibited versatile adhesion and creep resistance. Moreno and co-workers prepared lignin-based vitrimers by reacting lignin with poly(ethylene glycol) divinyl ether. The resulting materials demonstrated excellent relaxation rates facilitated by acetal exchange, leading to high mechanical performance [28]. However, these polymers exhibited a lap shear strength of 6 MPa, which is relatively low compared to commercial adhesives. Nevertheless, the specimens used in the lap shear tests could be easily reglued via hot pressing, achieving a lap shear strength of 5.6 MPa, highlighting the potential of these materials as recoverable adhesives. Our group described a family of recyclable and recoverable adhesives by changing proportions of DGEBA as epoxy monomer and glutaric anhydride and glycerol as co-curing agents [29]. All materials showed high T_g values and could relax the stress at high temperatures thanks to the transesterification reaction. Moreover, these epoxy vitrimers showed high values of lap-shear strength, and thanks to self-healable and viscoelastic properties of vitrimers at high temperatures, they could be dismantled and re-bonded again, demonstrating up to 89% of recovery concerning the first lap-shear value in one of the materials. However, these adhesives required high temperatures and a long time to be fully cured, which is a drawback from an industrial and energetical point of view.

The above-mentioned studies on adhesives have often relied on expensive and complex starting materials, involved complicated synthetic steps, required the use of costly metal catalysts, or had long and challenging curing parameters. These factors make them energetically unfeasible for industrial applications.

To address these issues, we present a study focusing on the development of two different adhesives using affordable and readily available diglycidyl ether of bisphenol A (DGEBA), pentaerythritol tetrakis (3-mercapto propionate) (S4), and dipentaerythritol hexakis (3-mercapto propionate) (S6) (see Scheme 1). We take advantage of the thiol-epoxy reaction with a click character that leads to the formation of hydroxyl groups that can undergo a further transesterification reaction with the esters present in the thiol monomer structure. In this work, we first select the appropriate catalyst and evaluate the evolution of the entire curing system using differential scanning calorimetry (DSC) and Fourier transform infrared spectroscopy (FTIR). The chosen catalyst and curing conditions are optimized for their viability in industrial production. The thermal stability of the resulting polymers was investigated using thermogravimetry (TGA), while their thermomechanical properties,

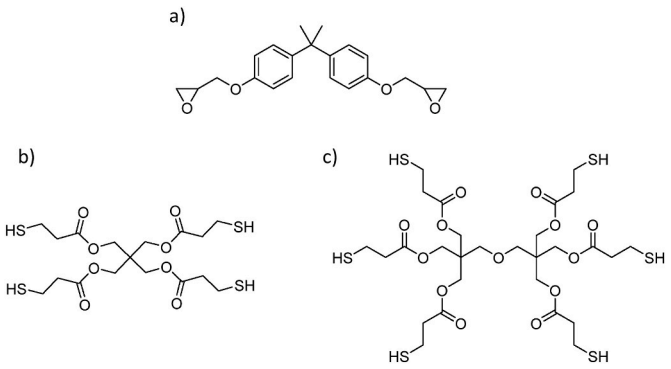

Scheme 1. Monomers used in the preparation of the materials a) DGEBA, b) S4 and c) S6.

vitrimeric behaviour, and creep resistance were characterized by dynamic-mechanical-thermal analysis (DMTA). Both materials exhibited stress relaxation at elevated temperatures and demonstrated resistance to creep at room temperature, enhancing their adhesive performance. Furthermore, tensile and lap-shear tests revealed high values of strength, thus highlighting the materials' promising adhesive properties. Additionally, the materials, which are transparent and colourless, exhibited shape-memory properties and the ability for permanent shape reconfiguration, opening up new possibilities for industrial applications. By utilizing cost-effective starting materials and demonstrating favourable properties and performance, these adhesives hold significant potential for practical industrial applications.

2. Experimental part

2.1. Materials

Diglycidyl ether of bisphenol A (DGEBA, 181.5 g/eq) was provided by Huntsman Corporation and dried in the vacuum for 2h at 80 °C. Pentaeryithrithol tetrakis (3-mercapto propionate) (S4, 98%, 122.17 g/eq) and dipentaerythrithol hexakis (3-mercapto propionate) (S6, 98%, 130.5g/eq) were supplied from Bruno Bock Thiochemicals and used as received. 1,5-Diazabicyclo[4.3.0]non-5-ene (DBN, 96%) and 1,8-diazabicyclo[5.4.0]undec-7-ene (DBU, >96%) were purchased at Alfa Aesar and Sodium tetraphenyl borate ($NaBPh_4$, 99%) at Thermo Scientific. 1-Methyl imidazole (1MI) and 2-methyl imidazole (2MI) were provided by BASF, and base generators of 1MI, DBN, and DBU were synthesized accordingly to the literature [30,31].

2.2. Preparation of the materials

When using liquid catalysts, a certain amount of DGEBA was added in a vial followed by the stoichiometric proportion of S4 or S6 (molar ratio epoxy:SH 1:1). Finally, a 1% mol or 5% mol (to SH) of the catalyst was added and vigorously stirred. Then, the prepared formulations were poured into rectangular Teflon moulds of 30 × 5 × 1.5 mm^3 dimensions and cured in a conventional oven at 80 °C for 4 h and at 120 °C for 2 h in the cases of S4 samples and 4 h at 120 °C for S6 samples.

In the case of solid catalysts, a 1% mol (to SH) of the catalyst was weighted on a vial followed by adding a certain amount of S4 or S6. Then, the mixture was kept at 80 °C for 2 h under stirring to dissolve the catalyst. Finally, the stoichiometric amount of DGEBA (molar ratio epoxy:SH 1:1) was added and vigorously stirred. After that, the sample preparation procedure was the same as explained above.

2.3. Methods

A differential scanning calorimeter (DSC) Mettler DSC3+ calibrated using an indium standard (heat flow calibration) and indium-lead-zinc

standard (temperature calibration) was used to analyze the curing evolution. Samples of approximately 5–10 mg were tested in aluminium pans with a pierced lid in a nitrogen atmosphere with a 50 mL/min gas flow. Dynamic studies were performed in a temperature range of 30–250 °C with a heating rate of 10 °C/min for calculating the enthalpy (ΔH) released during the curing of the samples, which is obtained by integration of the calorimetric signal using a straight baseline, with the help of the STARe software. To calculate the glass transition temperature (T_g), dynamic studies were done in a temperature range of 0–250 °C with a heating rate of 20 °C/min.

A Jasco FT/IR-680 Plus spectrometer equipped with an attenuated total reflection accessory (ATR) (Gloden Gate, Specac Ltd, Teknokroma) was used to record the FTIR spectra of the mixture before and after the curing procedure. Real-time spectra were recorded in the wavenumber range between 4000 and 600 cm^{-1} with a resolution of 4 cm^{-1} and averaged over 20 scans. The disappearance of the characteristic peak of the epoxy group at 915 cm^{-1} and the peak of SH groups at 2576 cm^{-1} as well as the appearance of the peak corresponding to O–H at 3300 cm^{-1} were used to confirm the completion of the reaction.

The thermal stability of the materials was evaluated using a Mettler Toledo TGA 2 thermobalance. Cured samples weighing around 10 mg were degraded between 30 and 600 °C at a heating rate of 10 °C/min under an N_2 atmosphere with a flow rate of 50 cm^3 min^{-1}.

The thermomechanical properties were studied using a DMTA Q800 (TA Instruments) equipped with a film tension clamp. Prismatic rectangular samples with dimensions of around 30 × 5 × 1.5 mm^3 were analyzed from 0 to 200 °C at 1 Hz, with 0.1% strain at a heating rate of 2 °C/min. Tensile stress-relaxation tests were conducted in the same instrument using the film tension clamp on samples with the same dimensions as previously defined. The samples were first equilibrated at the relaxation temperature for 5 min, and a constant strain of 1% was applied, measuring the consequent stress level as a function of time. The materials were tested only once at one temperature. The relaxation-stress $\sigma(t)$ was normalized by the initial stress σ_0, and the relaxation times (τ) were determined as the time necessary to relax $0.37\sigma_0$, i.e., ($\sigma = 1/e\sigma_0$). With the relaxation times obtained at each temperature, the activation energy values (E_a) were calculated using an Arrhenius-type equation:

$$\ln(\tau) = \frac{E_a}{RT} - \ln A$$

Where τ is the time needed to attain a given stress-relaxation value ($0.37\sigma_0$), A is the pre-exponential factor, and R is the gas constant. From Arrhenius relaxation, the topology freezing temperature (T_v) was obtained as the temperature at which the material reaches a viscosity of 10^{12} Pa s. Using Maxwell relation and E' determined from DMTA (assuming E' is relatively invariant in the rubbery state), τ^* was determined to be between 10^4 s and 10^5 in our systems. The Arrhenius relationship was then extrapolated to the corresponding value of τ^* to determine T_v in each sample.

Creep and recovery properties were studied by the same DMTA Q800 apparatus equipped with a film tension clamp. All the samples were stretched under a stress of 0.1 MPa at different temperatures for 30 min, then the stress was immediately released, and the sample was left to recover for 30 min. To determine the viscosity at each temperature needed for the representation of the Fragility Angell Plot, a series of creep experiments were carried out on films at temperatures between 100 and 180 °C, increasing 10 °C in each scan. To perform the tests, the selected sample was equilibrated for 3 min at the specific temperature, and then a stress level of 0.1 MPa was applied for 30 min. The viscosity $\boldsymbol{\eta}$ (Pa·s) was then derived from the slope of the graph strain-temperature and represented in front of T_g/T, thus obtaining the Angell Fragility Plot. The Tv can also be calculated from this graph assuming a viscosity of 10^{12} Pa s.

Final materials were tested until the break in tensile mode at room temperature using an electromechanical universal testing machine (UTM Shimadzu AGS-X) with a 10 kN load cell at 10 mm min-1 and using Type V samples with a thickness of 1 mm according to the ASTM D638-14 standard [32]. Three samples of each material were analyzed, and the results were averaged.

Aluminium platens 6060 T66 of 100 × 25 mm^2 with a thickness of 1.5 mm were used for lap-shear tests, according to the standard UNE-EN ISO 1465:2009 [33] (equivalent to ASTM D1002-10) [34]. The adhesion surfaces of the aluminium substrates were prepared following the UNE-EN ISO 13887:2004 [35] standard to ensure and durable joint. Overlapping regions were polished and degreased with acetone to remove any greasy impurities. Mechanical abrasion by sandpaper was performed to roughen the bond area. Surfaces were again degreased with acetone in order to remove any abrasion residue. The vitrimer adhesives were obtained by preparing the formulation in a vial and pouring it on the adhesion surface. Then, the upper aluminium sheet was placed, maintaining a bondline thickness of 2 mm with the help of Teflon spacers, and the joint was cured in the oven. An overlapping length of 12.5 mm was used according to UNE-EN ISO 1465:2009 standard. Tensile lap shear tests of the single-lap joint prepared with the different vitrimer adhesives were performed according to UNE-EN ISO 1465:2009 in the UTM at 1.3 mm min^{-1} crosshead speed. To test the reversibility of the adhesives after lap shear breakage, the substrates were re-united in an oven at 180 °C for 1 h applying a determined pressure. Furthermore, a manual dismantle was also made to the original samples at 180 °C and re-joint following the previously mentioned procedure. Dismantled samples and lap shear broken samples were re-tested again using the same conditions to obtain their new lap shear strength.

3. Results and discussion

3.1. Election of the catalyst

We prepared several formulations with different catalysts and loadings to determine the most suitable catalyst for the curing reaction. We first chose DBN and DBU as they are not only strong bases for the catalysis of the thiol-epoxy reaction but also reported catalysts for the further transesterification reaction at high temperatures [36]. Formulations of DGEBA, the stoichiometric amount of S4, and a 5% mol (to SH) of catalyst were prepared. However, when the latest was added, the thiol-epoxy reaction quickly started polymerizing in the same vial (see Figure S1a). For this reason, we decided to decrease the loading of the catalyst to 1% mol (to SH). Unfortunately, the same happened, which hinders the use of these catalysts to prepare these adhesives. Then, 2MI was tested because its secondary amine can be covalently bonded in the structure of the network, which prevents the evaporation of the catalyst at high temperatures during the stress relaxation tests. Nevertheless, 2MI requires the dissolution of the mixture in dichloromethane and its further evaporation, which complicates the whole procedure. To ensure the applicability of the vitrimers as adhesives, base generators of DBU (1,8-diazabicyclo[5.4.0]undec-7-ene) and DBN (1,5-diazabicyclo[4.3.0] non-5-ene), as well as 1MI (1-methylimidazole), were prepared according to the literature (see Experimental Part). These base generators were selected because they possess a high latency of the formulation at room temperature, which is essential for the practical use of the vitrimer as an adhesive. Interestingly, when exposed to high temperatures, these base generators release specific species that activate the curing process and facilitate the further exchange reaction. This thermal responsiveness allows the vitrimer adhesive to undergo crosslinking and structural rearrangement, enhancing its adhesive properties under elevated temperature conditions. The 1% mol (to SH) of base generators was weighted and homogenized with the thiol, followed by adding DGEBA and curing in the oven. As shown in Figure S1b, when BGDBU and BGDBN were used after long curing times at high temperatures, materials were not homogenous due to the poor miscibility of these catalysts

in the formulations. In the case of BG1MI, homogenous samples could be obtained, but they required high temperatures (post-curing at 160 °C) to be fully cured. Finally, a 5% mol of 1MI was added to the mixture, and after the curing process, materials with high transparency were obtained, indicating high homogeneity (see Figure S2). The ease of preparation was also evident during the experimental procedure. Based on these observations, 1MI was selected as the catalyst for the vitrimeric system. Its use facilitates the formation of a homogeneous and transparent vitrimer while ensuring a soft and straightforward preparation process.

3.2. Study of the curing process

Once selected 1MI as the curing and the transesterification catalyst, the curing procedure should be determined. DSC tests were performed to know the reaction's enthalpy and to identify possible side reactions. As seen in Fig. 1a, both formulations showed monomodal curves suggesting that no side reactions are taking place as expected by the click character of the thiol-epoxy reaction. Moreover, the curing enthalpy (ΔH) was between 120 kJ/eq and 130 kJ/eq, as reported previously by our group [37]. Considering these results, the curing temperatures and times were set up. In the case of DGEBA_S4, the onset of the peak starts at low temperatures so 80 °C and 4 h was selected as the curing schedule and a further post-curing at 120 °C during 1 h to ensure the reaction of the remaining epoxy groups.

To check the completion of the reaction, FTIR spectrum of the initial mixture and the final material were recorded (Fig. 1b). The disappearance of the epoxy band at 910 cm^{-1}, the vanishment of the band at 2576 cm^{-1} corresponding to the free thiols and the appearance of the characteristic hydroxyl band at 3300 cm^{-1} confirmed that the thiol-epoxy reaction was completed [38].

3.3. Thermal characterization of the materials

To study the thermal stability of both materials as well as to confirm that no degradability takes place when thermal tests are performed, thermogravimetric analysis (TGA) was used. Fig. 2 shows the TGA curves and their derivatives, and Table 1 summarizes the most significant thermogravimetric data.

As can be seen, both materials present similar degradation patterns and high onset temperatures. DTG curves show two main peaks, which can be ascribed to a first β-elimination of the esters present in the structure of the thiols followed by a degradation of the remaining polymeric matrix [39]. It is worth saying that DGEBA_S6 loses 2% of weight at 274.9 °C, which is slightly higher than DGEBA_S4 due to the higher cross-linking density that provides higher thermal stability. Moreover, the char residue at 600 °C is bigger when the hexathiol is used for the same reason previously mentioned.

The thermomechanical properties of the final materials were evaluated by DMTA analysis. Fig. 3 shows the evolution of the damping capacity (tan δ) and the storage modulus (E') with the temperature, and the data extracted are presented in Table 1. The results demonstrate that the DGEBA_S6 formulation exhibits a higher cross-linking density, leading to increased material rigidity and higher values of storage modulus (E') in the glassy state. Similarly, the high functionality of the hexathiol component contributes to higher values of E' in the rubbery state, reflecting the influence of cross-linking density on material stiffness.

Furthermore, both materials exhibit $T_{tan\ \delta}$ values (considered as the glass transition temperature, T_g) above room temperature. This suggests that when used as adhesives, these materials will remain rigid in the glassy state at room temperature, ensuring excellent mechanical performance. Additionally, the T_g values allow the curing process to be conducted at moderate temperatures. Moreover, the low values of the full width at half maximum (FWHM) indicate fast transitions and high homogeneity in the materials. This is attributed to the click nature of the thiol-epoxy reaction, which promotes efficient and uniform curing reactions, resulting in homogeneous material properties.

3.4. Study of the vitrimeric behaviour of the materials

The vitrimeric behaviour of the materials is achieved through the transesterification reaction catalyzed by 1MI at elevated temperatures. During the curing process, the thiolate species attacks the less hindered carbon of the epoxide, forming a thioether and a secondary alcohol. Since the thiol hardeners contain ester groups in their structure, the exchange reactions can occur through the attack of the secondary alcohol on the ester groups of the thiols. This exchange reaction enables the materials to exhibit vitrimeric properties.

To investigate the time and temperature-dependent relaxation of the materials and assess their vitrimeric properties, stress relaxation tests were performed using dynamic-mechanical-thermal analysis (DMTA) at different temperatures. The results are depicted in Fig. 4, and the most relevant data are summarized in Table 2. It is evident that both materials exhibit favourable vitrimeric properties, but the thiol structure significantly affects the relaxation capability. Specifically, DGEBA_S4 demonstrates complete stress relaxation at 180 °C in less than 13 min, whereas DGEBA_S6 requires 45 min at the same temperature. This discrepancy can be attributed to the lower cross-linking density of DGEBA_S4, which provides greater chain mobility and enhances the likelihood of transesterification exchange reactions taking place.

In vitrimers, a characteristic feature is the establishment of a linear

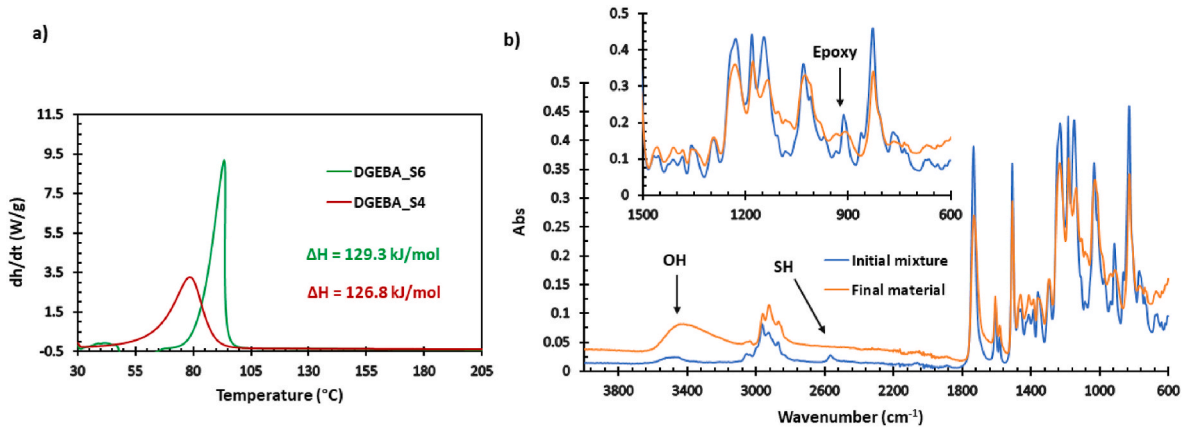

Fig. 1. a) DSC thermograms corresponding to the dynamic curing at 10 °C for DGEBA_S6 (green) and DGEBA_S4 (red) formulations b) FTIR spectra for the initial mixture (blue) and the final material (orange) for DGEBA_S4. (For interpretation of the references to colour in this figure legend, the reader is referred to the Web version of this article.)

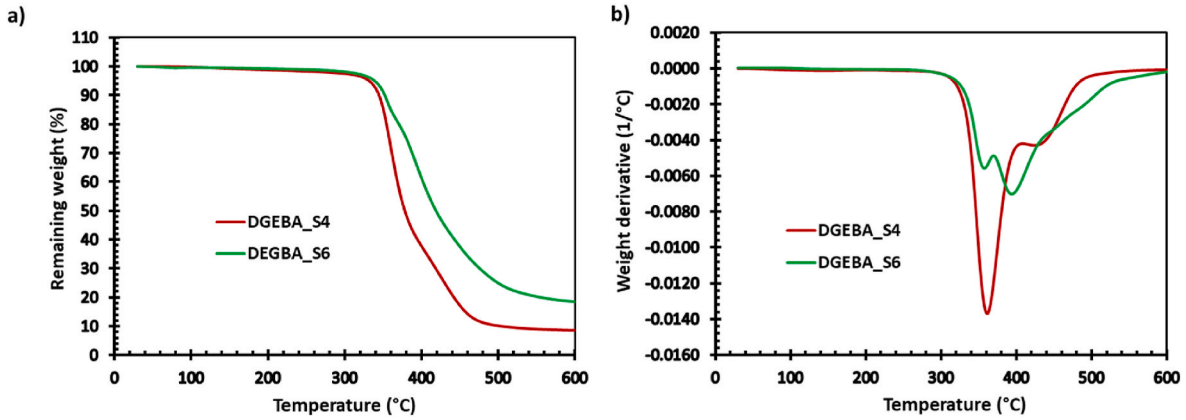

Fig. 2. a) Thermogravimetric curves and b) DTG curves of the vitrimeric materials.

Table 1
Thermogravimetric and thermomechanical data for both materials prepared.

Sample	$T_{2\%}$[a] (°C)	Char yield[b] (%)	E'_{glassy}[c] (MPa)	$E'_{rubbery}$[d] (MPa)	$T_{tan\delta}$[e](°C)	FWHM[f] (°C)
DGEBA_S4	266.2	9.0	2870	11.3	54.5	9.0
DGEBA_S6	274.9	18.1	3290	20.1	74.8	9.5

[a] Temperature of 2% of weight loss.
[b] Char residue at 600 °C.
[c] Glassy storage modulus at T_g −50 °C determined by DMTA.
[d] Rubbery storage modulus at T_g +50 °C determined by DMTA.
[e] Temperature at the maximum of tan δ peak at 1 Hz.
[f] Full width at the half medium of tan δ peak.

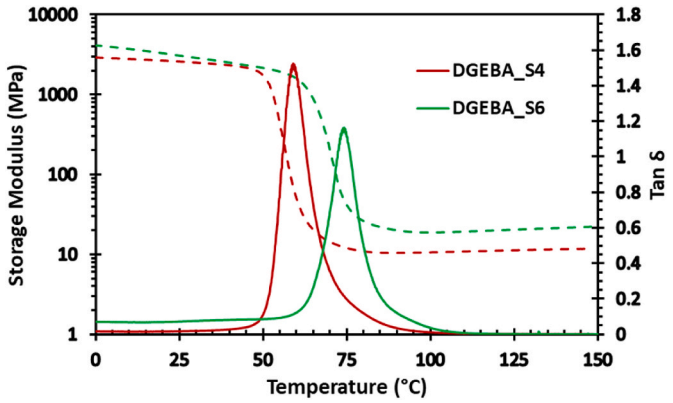

Fig. 3. Evolution of the storage modulus and tan δ with the temperature of both materials prepared.

relationship, akin to inorganic silica materials, between viscosity and temperature during exchange reactions. This behaviour follows an Arrhenius-type dependence [40]. To gain a deeper understanding of the vitrimeric behaviour exhibited by these materials, stress relaxation times required to achieve 37% of the initial stress ($\sigma/\sigma_0 = 0.37$) were determined at various temperatures, as shown in Fig. 4a and b. Using the Arrhenius equation, the activation energy (E_a) of the transesterification reaction and the ln A values for these materials were determined and presented in Table 2.

The obtained data reveal that both materials exhibit very similar values of activation energy (E_a). This finding is consistent with other transesterification vitrimers reported in the literature [20,21,41].

According to the Arrhenius equation, the topology freezing temperature (T_v) can be calculated. T_v is defined as the temperature at which the material reaches a viscosity of 10^{12} Pa s and can be considered as the approximate temperature at which chemical exchanges occur. Below T_v, the interchange mechanisms are almost negligible [20]. In our systems, both materials have T_v values higher than their respective T_g values, with DGEBA_S4 having a slightly lower T_v, likely due to its higher mobility. These T_v values suggest that the vitrimeric exchange is not expected to significantly affect the creep resistance of the adhesives at service temperatures. Thermomechanical tests were also conducted on samples that had undergone prolonged stress relaxation at high temperatures (180 °C). The resulting tan δ curves showed no notable changes, indicating that the topological structure of both materials remained unchanged before and after an extended relaxation process.

Creep tests were conducted in DMTA to investigate the effect of temperature on the viscosity of the materials and their vitrimeric behaviour. Fig. 5a and b shows the creep tests at different temperatures for DGEBA_S4 and DGEBA_S6 materials, respectively. Fig. 5c compares the creep behaviour at 150 °C. When the materials are subjected to constant stress above T_g but below T_v (70 °C), the strain is fully recovered, indicating that creep is almost negligible for both DGEBA_S4 and DGEBA_S6. However, as the temperature exceeds T_v and increases further, a notable increase in the slope of the ε-t curve is observed due to the decreasing viscosity of the material (inverse of the slope) with increasing temperature. Additionally, the occurrence of plastic deformation indicates the material's capability to undergo permanent reshaping. The creep behaviour observed in DGEBA_S6 exhibits a similar pattern to that of DGEBA_S4. However, there is a slight reduction in creep for DGEBA_S6 due to the higher crosslinking density resulting from incorporating the hexathiol compound. These findings indicate that DGEBA_S6 may serve as a superior adhesive, as it demonstrates the ability to maintain its properties across a broader temperature range without compromising its performance. The enhanced temperature stability of DGEBA_S6 also suggests its potential as a more versatile adhesive option.

The Angell fragility plot represented in Fig. 5d illustrates the vitrimer behaviour of both materials. As previously mentioned, upon surpassing the T_v, transesterification occurs, resulting in a gradual decrease in viscosity with increasing temperature, following an Arrhenius-type relationship. By utilizing the Angell fragility plot, it is possible to estimate the T_v by assuming a viscosity (η) of 10^{12} Pa s corresponding to a logarithm value of 12. The extracted data from the Angell Fragility plot are presented in Table 2, revealing a consistent trend in T_vs comparable to that obtained from stress relaxation tests.

3.5. Mechanical characterization

The mechanical properties of both materials were evaluated through stress-strain tests conducted at room temperature using a universal testing machine. The results for stress at break (σ_{break}), strain at break

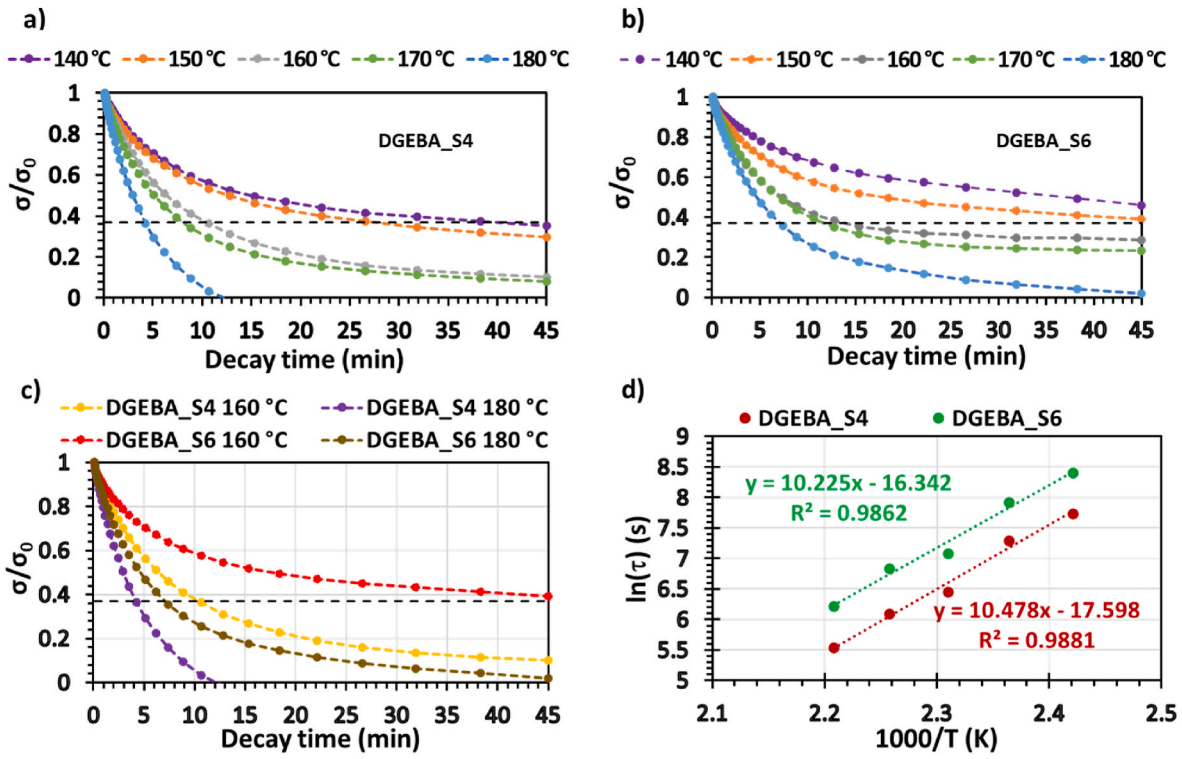

Fig. 4. Normalized stress-relaxation plots as a function of time at different temperatures during 45 min for DGEBA_S4 (a) and DGEBA_S6 (b). Normalized stress-relaxation behaviour at 160 °C and 180 °C for both samples (c) and Arrhenius plot of relaxation times against the inverse of temperature for both vitrimeric materials.

Table 2
Relaxation times, topology freezing temperature, activation energy and adjusting parameters for the Arrhenius equation, and topology freezing temperature and Fragility index from creep tests of both samples prepared.

	Stress relaxation tests						Creep tests	
Sample	$\tau_{0.37}$[a] (min)	$\tau_{100\%}$[b] (min)	E_a (kJ mol^{-1})	ln A (s)	T_v (°C)	r^2	$T_{v(\eta)}$[c] (°C)	n[d]
DGEBA_S4	4.3	12.2	87.0	17.6	89.1	0.988	84.6	8.2
DGEBA_S6	8.4	45.0	85.1	16.3	103.7	0.986	106.6	9.2

[a] Time to reach a value of $\sigma/\sigma_0 = 0.37$ at 180 °C.
[b] Time to reach total relaxation at 180 °C.
[c] T_v calculated by creep tests at different temperatures.
[d] Fragility index ($n_{silica} = 16.5$).

(ε_{break}), and tensile modulus (E) are collected in Table 3. As expected, DGEBA_S6 exhibits higher values of stress at break and tensile modulus compared to DGEBA_S4. This enhancement can be attributed to the elevated cross-linking density, which imparts greater strength to the material networks. Conversely, DGEBA_S4 demonstrates slightly higher values of strain at break due to the increased chain mobility, allowing for larger deformations.

3.6. Adhesion and re-adhesion properties

Adhesion lap-shear tests were conducted on both systems by joining aluminium plates following the UNE standard. The objective was to examine how the vitrimeric properties affect adhesion through re-adhesion tests involving dismantling and post-failure scenarios. In the dismantling test, the assembled joints were heated to 180 °C for 15 min, resulting in easy dismantling due to the occurrence of vitrimeric exchange reactions at that specific temperature. Subsequently, the fractured samples from the initial lap-shear test and the manually dismantled samples were re-joined by applying pressure and heating to 180 °C. It is important to note that a systematic investigation to determine the optimal conditions in temperature/time at which the joints can be dismantled and re-joined has not been performed. Thus, the temperatures (and times) were selected based on previous stress relaxation tests. The data obtained from the adhesion and re-adhesion tests are presented in Table 4, and the corresponding Force-displacement curves are presented in Figures S4-S6.

As shown in Table 4, the lap-shear values of the original joints are comparable to those of commercial adhesives with similar T_g (around 20 MPa), particularly for DGEBA_S4 [29,42]. However, the re-adhesion results after failure and after dismantling are significantly lower, but this can be explained by various factors. Upon the failure or dismantling of the adhesive joint, if the material distribution between the two plates is uneven, re-adhesion becomes challenging due to deficient surface preparation (such as roughening or the presence of dirt), resulting in suboptimal adhesion (see Figure S7). However, the joints have exhibited significant resistance despite this, suggesting potential for improvement through optimization and further experimentation in this test. Notably, upon examining the Force-displacement curves of the lap-shear tests (Figure S4-S6), it is evident that the initial slopes of the virgin, broken, and dismantled curves are highly similar. This suggests that the failure can be attributed to an experimental flaw in the joining process rather than being reflective of the material's inherent behaviour, as the trends

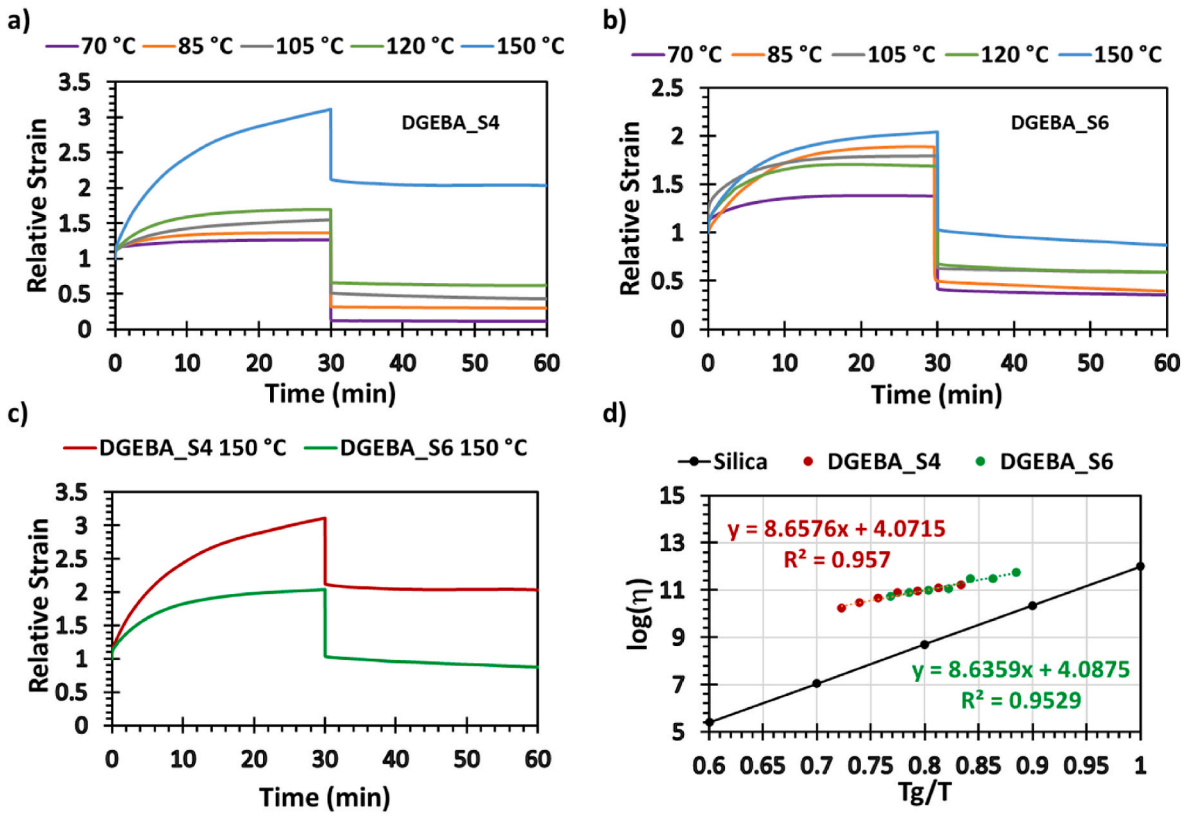

Fig. 5. Creep tests at different temperatures for DGEBA_S4 (a) and DGEBA_S6 (b). c) Comparison of the creep tests for both materials at 150 °C and d) Angell Fragility plot for both materials.

Table 3
Characteristic mechanical parameters obtained from tensile test measurements.

Sample	Young Modulus (MPa)	Absorbed energy (kJ/m^3)	σ_{break} (MPa)	ε_{break} (%)
DGEBA_S4	2345 ± 328	1119 ± 190	52.2 ± 3.8	3.9 ± 1.3
DGEBA_S6	2556 ± 152	896 ± 101	58.3 ± 4.0	2.8 ± 0.1

Table 4
Data extracted from adhesion and adhesion after failure and after dismantling tests.

	Virgin adhesion		Adhesion after failure		Adhesion after dismantling	
Material	F_{max} (N)	σ_{max} (MPa)	F_{max} (N)	σ_{max} (MPa)	F_{max} (N)	σ_{max} (MPa)
DGEBA_S4	5022 ± 220	16.1 ± 0.4	2017 ± 121	6.5 ± 0.3	2825 ± 89	9.0 ± 0.5
DGEBA_S6	3142 ± 301	10.1 ± 0.7	1745 ± 268	5.6 ± 0.4	2606 ± 159	8.3 ± 0.2

remain consistent across the different scenarios.

3.7. Reshaping, shape-memory and self-welding properties

A set of qualitative tests were conducted to demonstrate the reshaping capacity and shape memory properties of the materials, as depicted in Fig. 6.

In the case of vitrimers, where the T_v is significantly above the T_g, the material can exhibit shape-memory effect between T_g and T_v [18,21]. This means that if a temporary shape is imposed on the material at a temperature T within the range of $T_g < T < T_v$, and the material is rapidly cooled down, the original shape can be fully recovered by simply heating it above T_g. Conversely, if a shape is fixed at a temperature $T > T_v$, it will remain permanent due to the plastic deformation caused by the vitrimeric exchange. In Fig. 6a, a series of fixed temporary shapes at $T_g < T < T_v$ (A_P, B_P, C_P) are shown, which were successfully recovered by heating them above T_g (A_R, B_R, C_R). Additionally, plasticized shapes that were bent by annealing at $T > T_v$ for 60 min (B and C) are also illustrated. This cyclic process can be repeated multiple times due to the excellent thermal stability of the samples at these temperatures. It is noteworthy that the samples maintain good transparency throughout the treatments. Furthermore, Fig. 6b and c demonstrate the potential self-welding ability of these vitrimers, as the samples can be effectively joined together by heating them at temperatures above T_v (180 °C) for 1 h under sufficient pressure.

4. Conclusions

A series of functional adhesives derived from thermosetting polymers containing dynamic covalent bonds have been designed and fully characterized, offering significant potential for industrial applications. The reversible nature of these adhesives allows for reshaping, reprocessing, and recycling without causing damage to the substrate, thanks to the transesterification reaction responsible for their vitrimeric behaviour. Moreover, the materials are derived from easily accessible, cost-effective monomers (DGEBA, S4, and S6) and utilize a catalyst (1MI) that enables controlled curing parameters tailored to the specific materials being joined.

The vitrimeric adhesives exhibit high mechanical strength at room temperature, as evidenced by stress-strain tests with values of stress at break of 54 MPa and 73 MPa for DGEBA_S4 and DGEBA_S6, respectively. Notably, lap-shear tests demonstrate strong adhesion, especially for DGEBA_S4, yielding values of 16 MPa that are comparable to those of

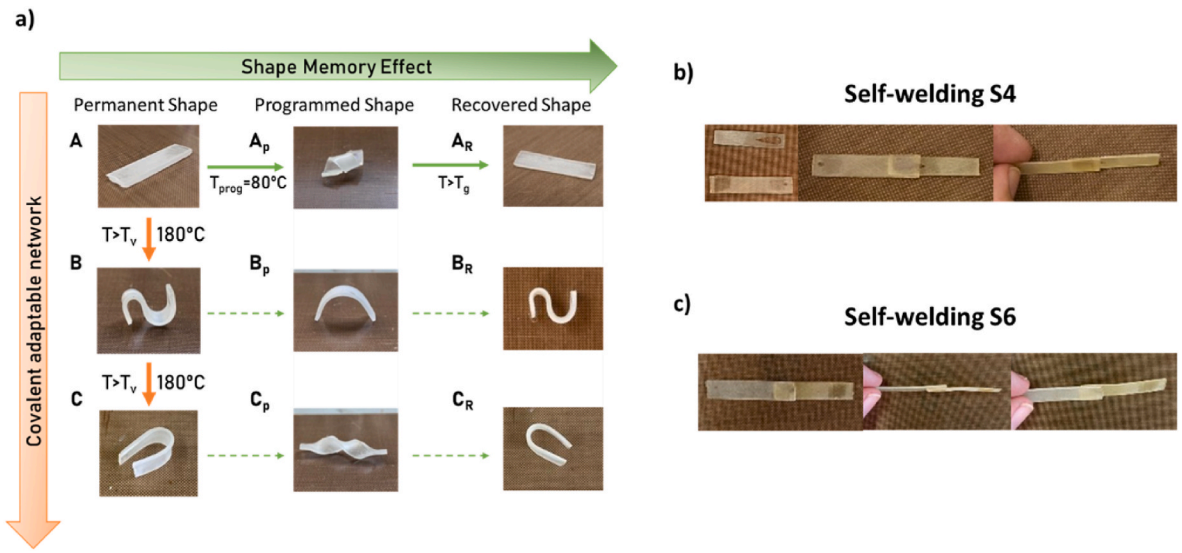

Fig. 6. a) Qualitative demonstration of shape memory behaviour and permanent/plastic shape change for DGEBA_S4 vitrimer. Pictures of the self-welding properties of DGEBA_S4 (b) and DGEBA_S6 (c).

other commercial adhesives.

The vitrimeric properties of the materials were further evaluated through stress relaxation tests at elevated temperatures, revealing topology freezing temperatures (T_vs) of 89 °C for DGEBA_S4 and 104 °C for DGEBA_S6. These temperatures ensure that the reprocessing of the materials does not compromise their mechanical properties. Creep tests indicate that both materials maintain mechanical integrity up to 70 °C, beyond which the exchange mechanisms begin to decrease the material's viscosity. Additionally, for DGEBA_S4 adhesive joints, efficient dismantling can be achieved at temperatures above 180 °C without causing damage to the substrates. However, it should be noted that the mechanical properties of the joints after failure and dismantling are significantly reduced due to the experimental re-adhesion procedure.

In conclusion, this study demonstrates that the developed materials possess not only the potential to be industrially competitive recyclable adhesives but also exhibit remarkable shape memory and self-welding properties. These findings highlight the significant potential of these materials in the industrial sector, showcasing their versatility and adaptability for various applications.

CRediT author statement

Adrià Roig conducted some experiments and wrote the original draft. Laura Molina performed some mechanical tests. David Santiago made adhesion tests. David Santiago and Silvia De la Flor made conceptualization and supervised the work. Àngels Serra, David Santiago and Silvia De la Flor reviewed and edited the final manuscript.

Declaration of competing interest

The authors declare that they have no known competing financial interests or personal relationships that could have appeared to influence the work reported in this paper.

Data availability

Data will be made available on request.

Acknowledgments

This work is part of the R&D projects PID2020-115102RB-C21 and TED2021-131102B–C22 funded by MCNI/AEI/10.13039/501100011033/Unión Europea NextGenerationEU/PRTR. The authors acknowledge these grants for their financial support. The authors also thank Generalitat de Catalunya (2021-SGR-00154). Huntsman and Bruno Bock Thiochemicals are also acknowledged for kindly giving us epoxy resin and thiol monomers, respectively.

Appendix A. Supplementary data

Supplementary data related to this article can be found at https://doi.org/10.1016/j.polymertesting.2023.108205.

References

[1] X. Luo, P.T. Mather, Shape memory assisted self-healing coating, ACS Macro Lett. 2 (2013) 152–156, https://doi.org/10.1021/mz400017x.
[2] J. Verrey, M.D. Wakeman, V. Michaud, J.A.E. Månson, Manufacturing cost comparison of thermoplastic and thermoset RTM for an automotive floor pan, Compos. Part A 37 (2006) 9–22, https://doi.org/10.1016/j.compositesa.2005.05.048.
[3] M. Giordano, A. Laudati, M. Russo, J. Nasser, G.V. Persiano, A. Cusano, Advanced cure monitoring by optoelectronic multifunction sensing system, Thin Solid Films 450 (2004) 191–194, https://doi.org/10.1016/j.tsf.2003.10.070.
[4] J. Economy, F.F. Shi, Aliphatic/aromatic copolyesters thermoset adhesives: synthesis and characterization, Polym. Eng. Sci. 37 (1997) 549–558, https://doi.org/10.1002/pen.11698.
[5] A. Kondyurin, Y. Klyachkin, Adhesion of UV-treated rubbers to epoxy adhesives, J. Appl. Polym. Sci. 62 (1996) 1–8.
[6] R. Avendaño, R.J.C. Carbas, E.A.S. Marques, L.F.M. da Silva, A.A. Fernandes, Effect of temperature and strain rate on single joints with dissimilar lightweight adherends bonded with an acrylic adhesive, Compos. Struct. 152 (2016) 34–44, https://doi.org/10.1016/j.compstruct.2016.05.034.
[7] M.Q. dos Reis, M.D. Banea, L.F.M. da Silva, R.J.C. Carbas, Mechanical characterization of a modern epoxy adhesive for automotive industry, J. Brazilian Soc. Mech. Sci. Eng. 41 (2019) 1–11, https://doi.org/10.1007/s40430-019-1844-2.
[8] L. Vertuccio, L. Guadagno, G. Spinelli, S. Russo, G. Iannuzzo, Effect of carbon nanotube and functionalized liquid rubber on mechanical and electrical properties of epoxy adhesives for aircraft structures, Compos. B Eng. 129 (2017) 1–10, https://doi.org/10.1016/j.compositesb.2017.07.021.
[9] I.A. Akpinar, K. Gültekin, S. Akpinar, H. Akbulut, A. Ozel, Research on strength of nanocomposite adhesively bonded composite joints, Compos. B Eng. 126 (2017) 143–152, https://doi.org/10.1016/j.compositesb.2017.06.016.
[10] G.M. Scheutz, J.J. Lessard, M.B. Sims, B.S. Sumerlin, Adaptable crosslinks in polymeric materials: resolving the intersection of thermoplastics and thermosets, J. Am. Chem. Soc. 141 (2019) 16181–16196, https://doi.org/10.1021/jacs.9b07922.
[11] M. Podgórski, B.D. Fairbanks, B.E. Kirkpatrick, M. McBride, A. Martinez, A. Dobson, N.J. Bongiardina, C.N. Bowman, Toward stimuli-responsive dynamic thermosets through continuous development and improvements in covalent adaptable networks (CANs), Adv. Mater. 32 (2020), 1906876, https://doi.org/10.1039/D0CS00452A.

[12] P. Taynton, K. Yu, R.K. Shoemaker, Y. Jin, H.J. Qi, W. Zhang, Heat- or water driven malleability in a highly recyclable covalent network polymer, Adv. Mater. 26 (2014) 3938–3942, https://doi.org/10.1002/adma.201400317.
[13] S. Wang, S. Ma, Q. Li, W. Yuan, B. Wang, J. Zhu, Robust, fire-safe, monomer recovery, highly malleable thermosets from renewable bioresources, Macromolecules 51 (2018) 8001–8012, https://doi.org/10.1021/acs.macromol.8b01601.
[14] A. Roig, P. Hidalgo, X. Ramis, S. De la Flor, À. Serra, Vitrimeric epoxy-amine polyimine networks based on a renewable vanillin derivative, ACS Appl. Polym. Mater. 4 (2022) 9341–9350, https://doi.org/10.1021/acsapm.2c01604.
[15] A. Roig, A. Petrauskaitė, X. Ramis, S. De la Flor, À. Serra, Synthesis and characterization of new bio-based poly(acylhydrazone) vanillin vitrimers, Polym. Chem. 13 (2022) 1510–1519, https://doi.org/10.1039/D1PY01694F.
[16] A. Rekondo, R. Martin, A. Ruiz de Luzuriaga, G. Cabañero, H.J. Grande, I. Odriozola, Catalyst-free room-temperature self-healing elastomers based on aromatic disulfide metathesis, Mater. Horiz. 1 (2014) 237–240, https://doi.org/10.1039/C3MH00061C.
[17] W. Denissen, M. Droesbeke, R. Nicolaÿ, L. Leibler, J.M. Winne, F.E. Du Prez, Chemical control of the viscoelastic properties of vinylogous urethane vitrimers, Nat. Commun. 8 (2017), 14857, https://doi.org/10.1038/ncomms14857.
[18] F. Gamardella, F. Guerrero, S. De la Flor, X. Ramis, A. Serra, A new class of vitrimers based on aliphatic poly(thiourethane) networks with shape memory and permanent shape reconfiguration, Eur. Polym. J. 122 (2020), 109361, https://doi.org/10.1016/j.eurpolymj.2019.109361.
[19] F. Van Lijsebetten, J.O. Holloway, J.M. Winne, F.E. Du Prez, Internal catalysis for dynamic covalent chemistry applications and polymer science, Chem. Soc. Rev. 49 (2020) 8425–8438, https://doi.org/10.1039/D0CS00452A.
[20] D. Montarnal, M. Capelot, F. Tournhilac, L. Leibler, Silica-like malleable materials from permanent organic networks, Science 334 (2011) 965–968, https://doi.org/10.1126/science.1212648.
[21] F.I. Altuna, C.E. Hoppe, R.J.J. Williams, Shape memory epoxy vitrimers based on DGEBA crosslinked with dicarboxylic acids and their blends with citric acid, RSC Adv. 6 (2016) 88647–88655, https://doi.org/10.1039/C6RA18010H.
[22] T. Liu, C. Hao, L. Wang, Y. Li, W. Liu, J. Xin, J. Zhang, Eugenol-derived biobased epoxy: shape memory, repairing and recyclability, Macromolecules 50 (2017) 8588–8597, https://doi.org/10.1021/acs.macromol.7b01889.
[23] E. Rosseger, R. Höller, D. Reisinger, J. Strasser, M. Fleisch, T. Griesser, S. Schlögl, Digital light processing 3D printing with thiol-acrylate vitrimers, Polym. Chem. 12 (2021) 639, https://doi.org/10.1039/D0PY01520B.
[24] M. Hayashi, A. Katayama, Preparation of colorless, highly transparent, epoxy-based vitrimers by the thiol-epoxy click reaction and evaluation of their shape-memory properties, ACS Appl. Polym. Mater. 2 (2020) 2452–2457, https://doi.org/10.1021/acsapm.0c00397.
[25] N.J. Van Zee, R. Nicolaÿ, Vitrimers: permanently crosslinked polymers with dynamic network topology, Prog. Polym. Sci. 104 (2020), 101233, https://doi.org/10.1016/j.progpolymsci.2020.101233.
[26] A. Trejo-Machin, L. Puchot, P.A. Verge, A cardanol-based polybenzoxazine vitrimer: recycling, reshaping and reversible adhesion, Polym. Chem. 11 (2020) 7026, https://doi.org/10.1039/D0PY01239D.
[27] L.M. Sridhar, M.O. Oster, D.E. Herr, J.B.D. Gregg, J.A. Wilson, A.T. Slark, Re-useable thermally reversible crosslinked adhesives from robust polyester and poly (ester urethane) Diels-Alder networks, Green Chem. 22 (2020) 8669–8679, https://doi.org/10.1039/D0GC02938F.
[28] A. Moreno, M. Morsali, M.H. Sipponen, Catalyst-free synthesis of lignin vitrimers with tunable mechanical properties: circular polymers and recoverable adhesives, ACS Appl. Mater. Interfaces 13 (2021) 57952–57961, https://doi.org/10.1021/acsami.1c17412.
[29] D. Santiago, D. Guzmán, J. Padilla, P. Verdugo, S. De la Flor, À. Serra, Recyclable and reprocessable epoxy vitrimer adhesives, ACS Appl. Polym. Mater. 5 (2023) 2006–2015, https://doi.org/10.1021/acsapm.2c02063.
[30] O. Konuray, N. Areny, J.M. Morancho, X. Fernández-Francos, A. Serra, X. Ramis, Preparation and characterization of dual-curable off-stoichiometric amine-epoxy thermosets with latent reactivity, Polymer 146 (2018) 42–52, https://doi.org/10.1016/j.polymer.2018.05.040.
[31] X. Sun, J.P. Gao, Z.Y. Wang, Bicyclic guanidinium tetraphenylborate: a photobase generator and a photocatalyst for living anionic ring-opening polymerization and cross-linking of polymeric materials containing ester and hydroxy groups, J. Am. Chem. Soc. 130 (2008) 8130–8131, https://doi.org/10.1021/ja802816g.
[32] Astm D638-14, Standard Test Method for Tensile Properties of Plastics, 2014.
[33] Une-En Iso 1465, Adhesives. Determination of Tensile Lap-Shear Strength of Bonded Assemblies, 2009.
[34] Astm D1002-10, Standard Test Method for Apparent Shear Strength of Single-Lap-Joint Adhesively Bonded Metal Specimens by Tension Loading (Metal-To-Metal), 2010.
[35] I.S.O. Une-En, Structural Adhesives. Guideline for Surface Preparation of Metals and Plastics Prior to Adhesive Bonding, 2004, 13887.
[36] H. Song, Z. Fang, B. Jin, P. Pan, Q. Zhao, T. Xie, Synergetic chemical and physical programming for reversible shape memory effect in a dynamic covalent network with two crystalline phases, ACS Macro Lett. 8 (2019) 682–686, https://doi.org/10.1021/acsmacrolett.9b00291.
[37] D. Guzmán, X. Ramis, X. Fernández-Francos, A. Serra, New catalysts for diglycidyl ether of bisphenol A curing based on thiol-epoxy click reaction, Eur. Polym. J. 59 (2014) 377–386, https://doi.org/10.1016/j.eurpolymj.2014.08.001.
[38] E. Pretsch, P. Bühlmann, M. Badertscher, Structure Determination of Organic Compounds: Tables of Spectral Data; 4th Ed, Springer Berlin, Heidelberg, 2009.
[39] M. Arasa, X. Ramis, J.M. Salla, A. Mantecón, A. Serra, A study of the degradation of ester-modified epoxy resins obtained by cationic copolymerization of DGEBA with -lactones initiated by rare earth triflates, Polym. Degrad. Stabil. 92 (2007) 2214–2222, https://doi.org/10.1016/j.polymdegradstab.2007.01.037.
[40] W. Denissen, J.M. Winne, F.E. Du Prez, Vitrimers: permanent organic networks with glass-like fluidity, Chem. Sci. 7 (2016) 30–38, https://doi.org/10.1039/C5SC02223A.
[41] M. Capelot, M.M. Unterlass, F. Tournilhac, L. Leibler, Catalytic control of the vitrimer glass transition, ACS Macro Lett. 1 (2012) 789–792, https://doi.org/10.1021/mz300239f.
[42] C. Russo, F. Bustamante, X. Fernández-Francos, S. De la Flor, Adhesive properties of thiol-acrylate-epoxy composites obtained by dual-curing procedures, Int. J. Adhesion Adhes. 112 (2022), 102595, https://doi.org/10.1016/j.ijadhadh.2021.102959.